LETTERS

Human-specific transcriptional regulation of CNS development genes by FOXP2

Genevieve Konopka[1,3], Jamee M. Bomar[1,3], Kellen Winden[1,3], Giovanni Coppola[3], Zophonias O. Jonsson[5], Fuying Gao[3], Sophia Peng[3], Todd M. Preuss[6], James A. Wohlschlegel[5] & Daniel H. Geschwind[1,2,3,4]

The signalling pathways controlling both the evolution and development of language in the human brain remain unknown. So far, the transcription factor *FOXP2* (forkhead box P2) is the only gene implicated in Mendelian forms of human speech and language dysfunction[1–3]. It has been proposed that the amino acid composition in the human variant of FOXP2 has undergone accelerated evolution, and this two-amino-acid change occurred around the time of language emergence in humans[4,5]. However, this remains controversial, and whether the acquisition of these amino acids in human FOXP2 has any functional consequence in human neurons remains untested. Here we demonstrate that these two human-specific amino acids alter FOXP2 function by conferring differential transcriptional regulation *in vitro*. We extend these observations *in vivo* to human and chimpanzee brain, and use network analysis to identify novel relationships among the differentially expressed genes. These data provide experimental support for the functional relevance of changes in FOXP2 that occur on the human lineage, highlighting specific pathways with direct consequences for human brain development and disease in the central nervous system (CNS). Because FOXP2 has an important role in speech and language in humans, the identified targets may have a critical function in the development and evolution of language circuitry in humans.

The amino acid structure of FOXP2 had been highly conserved along the mammalian lineage until the common ancestor of humans and chimpanzees, when the human variant of FOXP2 acquired two different amino acids under positive selection, which has been interpreted as evidence for accelerated evolution[4,5]. To test whether the amino acids under positive selection in human FOXP2 have a distinct biological function, which would support the role of these changes in evolution, we expressed either human FOXP2 or the same construct mutated at two sites to yield the chimpanzee amino acid content, $FOXP2^{chimp}$, in human neuronal cells without endogenous FOXP2 (Fig. 1a–f). Exogenous FOXP2 protein expressed from both constructs was localized in the nucleus as determined by immunocytochemistry (Fig. 1c–e) and subcellular fractionation (Fig. 1f), consistent with its endogenous expression. To determine if modifying two amino acids leads to changes in gene expression, we conducted whole-genome microarray analysis. We identified 61 genes significantly upregulated and 55 genes downregulated by FOXP2 compared to $FOXP2^{chimp}$ (Supplementary Table 1), as well as genes regulated by both FOXP2 and $FOXP2^{chimp}$ (Supplementary Table 2). Notably, $FOXP2^{chimp}$ overexpression resulted in more changes in gene regulation than FOXP2 (Supplementary Table 3). In replicate experiments in a different human neuronal cell line, $FOXP2^{chimp}$ again regulated more genes than FOXP2 even though its expression was higher than FOXP2 in these cells (data not shown). To control for any potential confounding effects of FOXP2 levels, we performed correlations of the levels of every gene on the array to either FOXP2 or $FOXP2^{chimp}$ levels, as well as performing random permutation testing, and found no significant differences between other genes' correlations to either FOXP2 or $FOXP2^{chimp}$. These data indicate that the differentially expressed genes are not due to different levels of FOXP2 or $FOXP2^{chimp}$, and are a true indication of differential transcriptional regulation by these two proteins.

To confirm the validity of differentially expressed FOXP2 target genes, we conducted quantitative polymerase chain reaction following reverse transcription (qRT–PCR) using independent RNA samples. We confirmed 93% of the FOXP2 upregulated genes and 75% of the downregulated genes examined (Fig. 1g, h and Supplementary Fig. 1). Five genes confirmed by qRT–PCR (*COL9A1*, *ROR2*, *SLIT1*, *SYK*, and *TAGLN*; Fig. 1g, h and Supplementary Fig. 1) were previously identified as direct FOXP2 targets using ChIP-chip[6,7]. Sixty per cent of promoters of the identified differentially expressed genes have at least one canonical FOXP2 binding site, 92% have at least one forkhead domain binding site, and 99% have at least one 'core' FOXP2 binding site (Supplementary Table 4). The canonical FOXP2 binding site CAAATT, as well as the core site AAAT, is significantly enriched in the downregulated genes ($P = 3.3 \times 10^{-4}$ and $P = 8.6 \times 10^{-3}$, respectively) compared to randomly permuting the same number of promoters from the genome. Genes with promoters containing a canonical FOXP2 binding site are likely to be direct FOXP2 or $FOXP2^{chimp}$ targets.

To confirm that these findings were not an artefact of the cell lines used, we further assessed whether a different primary neural cell, human neural progenitors, would show similar differential regulation by FOXP2 and $FOXP2^{chimp}$. We confirmed one-third of the genes examined in these human cells using both a different method of gene transduction, and populations of cells with greater levels of $FOXP2^{chimp}$ compared to human FOXP2 overexpression, which complements the SH-SY5Y data to further show that the observed relationships are not due to FOXP2 levels (Supplementary Fig. 2). As an additional level of validation and to extend the findings to the level of protein, we confirmed two genes, *CACNB2* and *ENPP2*, by immunoblotting in additional SH-SY5Y cell lines (Supplementary Fig. 3).

To explore the potential function of the differential FOXP2 targets, we determined enrichment of gene ontology (GO) categories. GO categories enriched for genes upregulated by FOXP2 compared to $FOXP2^{chimp}$ are involved in transcriptional regulation of gene expression and cell–cell signalling. Those GO categories enriched for genes downregulated by FOXP2 compared to $FOXP2^{chimp}$ are important for protein and cell regulation (Supplementary Table 5).

[1]Program in Neurogenetics, [2]Semel Institute and Department of Psychiatry, [3]Departments of Neurology, [4]Human Genetics, and [5]Biological Chemistry, David Geffen School of Medicine, University of California, Los Angeles, California 90095, USA. [6]Division of Neuroscience and Center for Behavioral Neuroscience, Yerkes National Primate Research Center, and Department of Pathology & Laboratory Medicine, Emory University School of Medicine, Atlanta, Georgia 30329, USA.

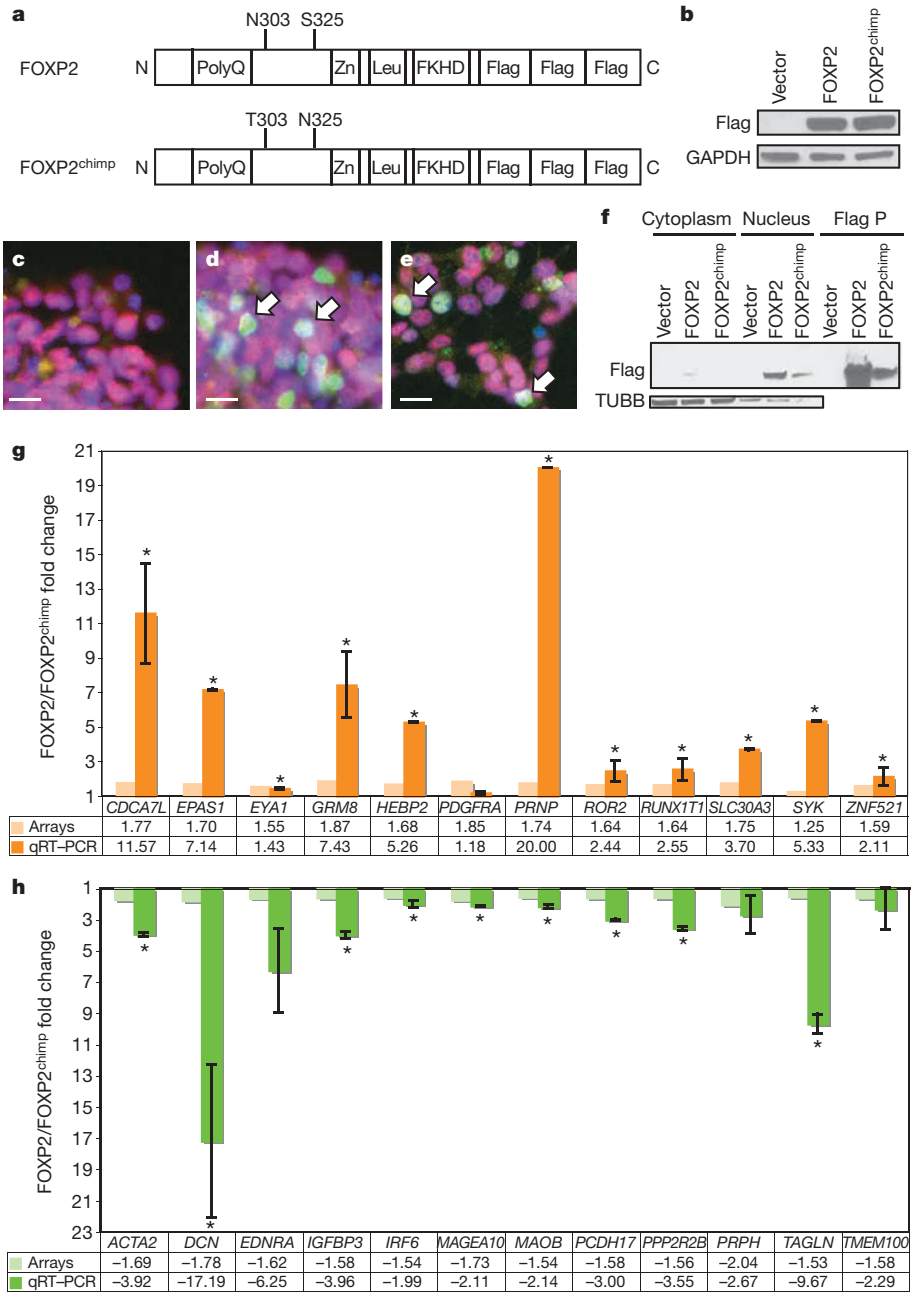

Figure 1 | FOXP2 and FOXP2^{chimp} differentially regulate genes in SH-SY5Y cells. **a**, Schematic of human FOXP2 showing its major functional protein domains (Zn indicates the zinc finger domain, Leu indicates the leucine-zipper domain, and FKHD indicates the forkhead DNA binding domain) and the two amino acid changes in the mutant FOXP2^{chimp}. **b**, Representative immunoblot for Flag-tagged FOXP2 and FOXP2^{chimp} stable overexpression in SH-SY5Y cells. **c–e**, Immunofluorescent staining of antibodies against Flag epitope (green) and FOXP1 (red), and 4,6-diamidino-2-phenylindole (DAPI; blue) for nuclei. Vector cells demonstrate no Flag expression (**c**), whereas both FOXP2 (**d**) and FOXP2^{chimp} (**e**) expressing cells have Flag-tagged FOXP2 in the cell nucleus. Arrows indicate examples of cell nuclei positive for Flag expression. Scale bars, 5 μm. **f**, Subcellular fractionation followed by immunoblotting. **g**, **h**, Quantitative RT–PCR of genes that were differentially expressed in cells expressing FOXP2 compared to FOXP2^{chimp}. Asterisks indicate $P \leq 0.05$ and error bars are ± s.e.m. (two-tailed Student's *t*-test, $n = 3$ or 4).

These data support the idea that FOXP2 and FOXP2^{chimp} have distinguishable downstream effects as reflected by their differences in gene regulation.

To determine the potential mechanisms by which FOXP2 or FOXP2^{chimp} might differentially regulate gene expression, we first examined whether either protein preferentially interacts with FOXP1 or FOXP4, two proteins known to form a heterodimer with FOXP2 (ref. 8). Both FOXP2 and FOXP2^{chimp} co-localized with FOXP1 in the cell nucleus, co-immunoprecipitated with FOXP1 as evidenced by immunoblotting, and co-immunoprecipitated with both FOXP1 and FOXP4 when assayed by mass spectrometry (Figs 1c–e, 2a, b and Supplementary Fig. 4b–g), ruling out a major difference in FOXP1 or FOXP4 interaction causing differential gene expression. Mass spectrometry showed no significant difference in either co-immunoprecipitation experiment, indicating that differences in hetero- or homodimerization did not underlie the observed differences in gene expression between the chimpanzee and human FOXP2. We also tested whether changes in cell proliferation could account for gene expression differences, but did not find significant changes in growth with either FOXP2 construct (Fig. 2c).

We next assessed whether FOXP2 and FOXP2^{chimp} expression led to differential promoter transactivation of target genes. We selected eight genes confirmed by qRT–PCR that also contained at least one forkhead binding site (Supplementary Table 6). Six of the promoters

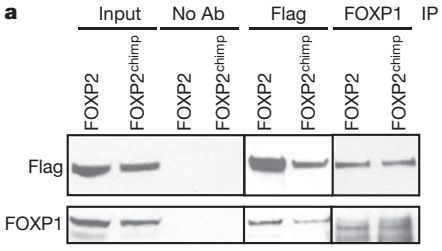

b

		FOXP2	FOXP1	FOXP4
SH-SY5Y	FOXP2	65/16	34/11	15/9
SH-SY5Y	FOXP2chimp	29/11	11/8	2/2
293T	FOXP2	32/10	5/4	6/5
293T	FOXP2chimp	106/23	18/11	21/10

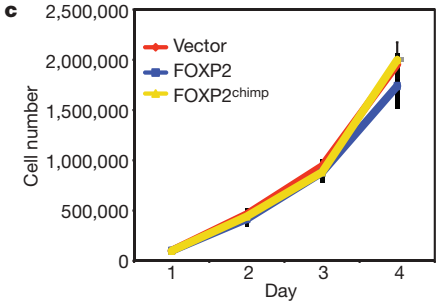

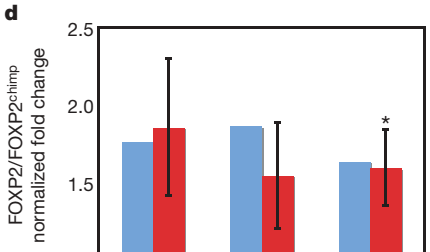

	CDCA7L	GRM8	ROR2
Arrays	1.77	1.87	1.64
Luciferase	1.86	1.55	1.60

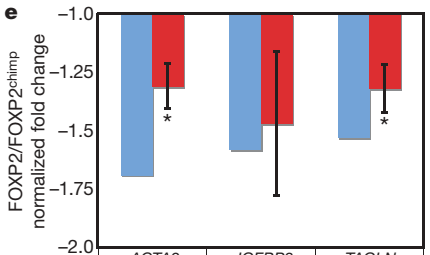

	ACTA2	IGFBP3	TAGLN
Arrays	−1.69	−1.58	−1.53
Luciferase	−1.31	−1.47	−1.32

Figure 2 | FOXP2 and FOXP2^{chimp} differentially transactivate target promoters independent of FOXP1 or FOXP4 interaction. **a**, Immunoblotting for Flag or FOXP1 following immunoprecipitation with either Flag or FOXP1 antibodies. **b**, Mass spectrometry results from SH-SY5Y or 293T cells overexpressing FOXP2 or FOXP2^{chimp}. The first number indicates the number of spectra and the second is the number of unique peptides. **c**, Cell growth analysis does not show a significant difference in proliferation between cells expressing FOXP2 or FOXP2^{chimp} over time ($P \leq 0.05$). Error bars are ± s.e.m. (two-tailed Student's *t*-test, $n = 3$). **d**, **e**, Dual luciferase assays in 293T cells transiently transfected with promoter fragments driving luciferase and either FOXP2 or FOXP2^{chimp}. Asterisks indicate $P \leq 0.05$ and error bars are ± s.e.m. (two-tailed Student's *t*-test, $n = 3$–6).

tested showed differential regulation by FOXP2 compared to FOXP2^{chimp} in the same direction as the microarrays (Fig. 2d, e), whereas two did not demonstrate significant transactivation in either direction (data not shown). In contrast, a canonical FOXP2 binding site in triplicate alone, outside of a genomic context, was regulated equally by both FOXP2 and FOXP2^{chimp} (Supplementary Fig. 5). Given the complexity of *cis*-acting gene transactivation elements, these data are particularly compelling considering our use of simplified 5′ promoter regions. These data demonstrate that at least a subset of differentially regulated genes is also differentially transactivated by FOXP2 and FOXP2^{chimp}, indicating that they are probably direct FOXP2 targets.

To place these gene expression changes within a more systematic context, we applied weighted gene co-expression network analysis[9,10] to the entire SH-SY5Y microarray data set to examine co-regulation of gene expression across all genes. We uncovered two modules where the module eigengene (for definition, see Methods) was driven by differences in FOXP2 and FOXP2^{chimp}, and one module driven by similar gene regulation (Fig. 3 and Supplementary Fig. 6). Using this unsupervised analysis, we found additional genes of interest that do not meet the criteria for differential expression, but that are co-regulated with differences in FOXP2 and FOXP2^{chimp} expression (Supplementary Table 7). Notably, two of the genes with the most connections, so-called 'hub' genes, in one of the differential networks are *DLX5* and *SYT4*, two genes important for brain development and function[11,12].

To extrapolate these findings to true *in vivo* expression and provide external validation, we compared the differentially expressed genes in SH-SY5Y cells to differentially expressed genes from adult human and chimpanzee brain tissue. We performed microarray analysis on tissue from three brain regions where FOXP2 is expressed in developing brain: caudate nucleus, frontal pole and hippocampus. We examined gene expression in human compared to chimpanzee for each brain region separately as well as for all brain regions combined, for a total of eight comparisons. There was a significant overlap in seven out of eight of these comparisons, a remarkable convergence with the *in vitro* data (Table 1). These data are particularly notable, as the tissue was from adult brain. We surmise that a subset of the overlapping differentially expressed genes found in adult brain is the result of differential functions by FOXP2 in the developing brain, and may lead to increased vulnerability to disease. For example, mutations in both *FGF14* and *PPP2R2B* lead to spinocerebellar ataxia (spinocerebellar ataxia type 27 and 12, respectively), which involves motor-related speech defects[13,14]. Because both of these genes have a critical role in cerebellar function, it is of note that patients with FOXP2 mutations have decreased grey matter in the cerebellum[15], and *Foxp2* knockout mice have their most pronounced morphological phenotype in the cerebellum[16]. Mutations in *COL9A1* lead to Stickler syndrome in which patients have craniofacial abnormalities[17], and patients with mutations in *GJA12* (also called *GJC2*) present with ataxia, nystagmus, other motor impairments, and often mental retardation[18].

Although comparisons of developing brain between human and chimpanzee are challenged by a lack of tissue, a recent study examined gene expression in many regions of human fetal brain[19]. Comparing the list of 116 differentially expressed genes with those focally expressed during human fetal development, we find 14 genes specifically expressed in one brain region, including FOXP2 (Supplementary Table 8). Two regions of the human fetal brain with high FOXP2 expression[19]—perisylvian cortex and cerebellum—have a significant number of enriched genes that overlap with the differentially expressed FOXP2 and FOXP2^{chimp} genes ($P = 1.1 \times 10^{-4}$ and $P = 1.3 \times 10^{-4}$, respectively; Supplementary Table 8). A significant number of the differentially expressed genes are also associated with human-specific accelerated highly conserved non-coding sequences (haCNS), but not with chimpanzee highly conserved non-coding sequences ($P = 1.2 \times 10^{-6}$ and $P = 0.04$; Supplementary Table 8)[19,20]. We confirmed a number of these genes, such as *GRM8*, *MAOB*, *PPP2R2B*, *PRICKLE1* and *RUNX1T1*, either by qRT–PCR and/or with the adult *in vivo* data set (Fig. 1 and Table 1). Together, these data suggest that the FOXP2 differentially expressed genes identified here may have important roles in brain development and patterning, and may also have evolved *cis*-regulatory elements important for their expression specifically in human brain.

Previously, we identified ChIP-chip targets of FOXP2 that themselves were also under positive selection[6]. We hypothesized that networks of genes important for language circuitry had been positively selected through selective pressure on human brain evolution. Thus, we also examined whether any differential FOXP2 targets were themselves

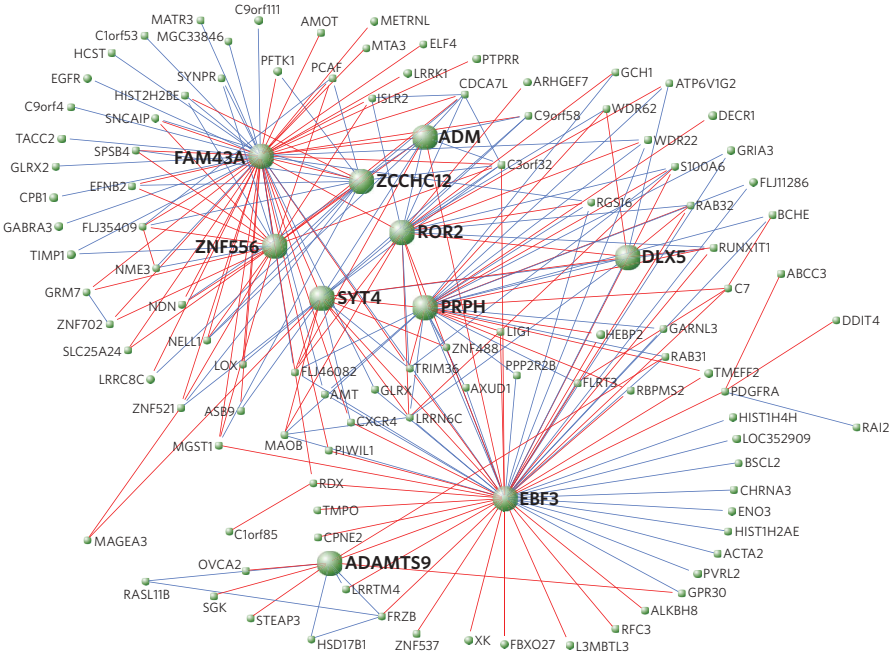

Figure 3 | Visualization of one of the modules containing FOXP2 and FOXP2^{chimp} differentially expressed genes. Two-hundred-and-fifty pairs of genes with the greatest topological overlap are shown. Positive correlations are depicted in red and negative correlations are depicted in blue. The gene symbols for hub genes are accentuated in large, bold text.

under positive selection. Five genes (*AMT*, *C6orf48*, *MAGEA10*, *PHACTR2* and *SH3PXD2B*) met the standard criteria of $K_a/K_s \geq 1.0$ for positive selection on the human lineage (where K_a indicates the rate of non-synonymous substitutions and K_s indicates the rate of synonymous substitutions; Supplementary Table 9)[21]. These data, along with the haCNS and expression data mentioned above, suggest that a subset of differential FOXP2 targets may have co-evolved to regulate pathways involved in higher cognitive functions.

The positive selection of two amino acids in human FOXP2 was previously hypothesized as a mechanism by which human FOXP2 might assume a novel biological function with implications for speech and language evolution[4,5]. A recent study made an elegant attempt to examine the role of these two amino acids by generating a transgenic mouse with the human version of FOXP2 (ref. 22). These mice show a number of interesting phenotypic alterations including increases in dendritic length in striatal neurons and changes in

Table 1 | Overlap of cell and *in vivo* microarray data

Genes	Cells	All brain areas (7.36×10^{-4} upregulated; 1.10×10^{-6} downregulated)*	Hippocampus (4.49×10^{-2} upregulated; 4.07×10^{-8} downregulated)*	Caudate (4.04×10^{-2} upregulated; 2.86×10^{-2} downregulated)*	Frontal pole (7.21×10^{-2} upregulated; 1.86×10^{-4} downregulated)*
Upregulated					
ADAMTS9	1.38	1.91	1.72	2.35	1.73
BCAN	1.29	–	–	1.64	–
COL9A1	1.26	1.23	–	1.26	–
EXPH5	1.27	1.41	1.29	1.43	1.53
FRZB	1.32	1.65	1.39	2.04	1.57
IGFBP4	1.27	1.35	–	–	1.59
ISLR2	1.30	1.27	1.53	–	–
MGST1	1.26	2.33	1.79	3.34	2.13
NPTX2	1.24	1.28	–	1.46	–
PDGFRA	1.84	1.27	–	1.35	–
PRICKLE1	1.45	–	1.43	–	–
RUNX1T1	1.64	1.24	1.33	–	1.24
SLC30A3	1.75	1.92	2.20	1.83	1.74
Downregulated					
ACCN2	−1.27	−1.33	−1.31	−1.28	−1.39
B3GNT1	−1.24	−1.73	−1.47	−2.55	−1.39
C6orf48	−1.23	−1.56	−1.53	−1.65	−1.51
C8orf13	−1.27	−1.36	−1.64	–	−1.29
CACNB2	−1.23	−1.69	−1.4	−2.58	−1.35
DCN	−1.78	−1.39	−1.68	–	−1.33
ELMO1	−1.28	−1.34	–	−1.64	−1.32
ENPP2	−1.39	−1.43	−1.72	–	–
FAM43A	−1.40	–	−1.32	–	–
FAM43B	−1.40	–	–	–	−1.41
FGF14	−1.23	−1.34	−1.24	−1.57	
FLJ11286	−1.27	−1.38	−1.32	−1.31	−1.51
GJA12	−1.25	−1.35	–	–	–
GLRX	−1.29	–	–	−1.30	–
HIST2H2BE	−1.30	−1.39	−1.61	–	−1.39
IFIT2	−1.24	−1.34	−1.49	–	–
IGFBP3	−1.58	–	−1.30	–	–
MAOB	−1.54	–	−1.26	–	–
PPP2R2B	−1.56	−1.23	−1.66	−1.35	−1.41

* Overlap *P* values for upregulated and downregulated genes are given in parentheses.

ultrasonic vocalizations, as well as some modest changes in gene expression. Although the mouse is an experimentally tractable model system, from a strictly evolutionary standpoint, the interpretation of data obtained in the mouse specifically for the study of human evolution is challenged by the vast differences in human and mouse brain and the amount of time since the human and mouse common ancestor diverged (70 million years[23]). Here, we demonstrate that these two amino acid changes have a functional consequence in human cells, validate these differences *in vivo* in tissue, and elucidate some of the downstream pathways affected by this adaptive evolutionary change.

Using whole-genome microarrays, we uncovered genes that are differentially regulated upon mutation of these two amino acids, including some with functions critical to the development of the human central nervous system. Moreover, this study reveals enrichment of differential FOXP2 targets with known involvement in cerebellar motor function, craniofacial formation, and cartilage and connective tissue formation, suggesting an important role for human FOXP2 in establishing both the neural circuitry and physical structures needed for spoken language. The significant overlap of human FOXP2 targets in cell lines with genes enriched in human compared to chimpanzee brain tissue presents the possibility that human and chimpanzee FOXP2 have differentially regulated targets during brain development. As suggested over 30 years ago[24], and reaffirmed by the sequencing of both the human and chimpanzee genomes, the phenotypic differences exhibited by humans and chimpanzees cannot be explained by differences in DNA sequence alone, and are probably due to differences in gene expression and regulation. Previous microarray studies identified differences in gene expression between human and chimpanzee brains[25,26]. Here, we link new whole-genome expression microarray data from human and chimpanzee brain to direct differences in gene regulation by the human and chimpanzee version of the transcription factor FOXP2. Because normal FOXP2 function is critical for speech in humans, these differentially regulated targets may be relevant to the evolution and establishment or function of pathways necessary for speech and language in humans.

METHODS SUMMARY

Cell culture and stable line generation. SH-SY5Y cells (ATCC) and human fetal neuronal progenitors (Lonza) were grown according to the manufacturer's instructions, with some modifications (see Methods).

Microarrays. Total RNA was extracted using Qiagen's RNeasy kit. Illumina HumanRef-8 v2 (SH-SY5Y samples) or v3 (tissue samples) were used and analysed as described[27]. Sample information is in Methods.

Full Methods and any associated references are available in the online version of the paper at www.nature.com/nature.

Received 26 August; accepted 1 October 2009.

1. Feuk, L. *et al.* Absence of a paternally inherited FOXP2 gene in developmental verbal dyspraxia. *Am. J. Hum. Genet.* **79,** 965–972 (2006).
2. Lai, C. S., Fisher, S. E., Hurst, J. A., Vargha-Khadem, F. & Monaco, A. P. A forkhead-domain gene is mutated in a severe speech and language disorder. *Nature* **413,** 519–523 (2001).
3. MacDermot, K. D. *et al.* Identification of FOXP2 truncation as a novel cause of developmental speech and language deficits. *Am. J. Hum. Genet.* **76,** 1074–1080 (2005).
4. Enard, W. *et al.* Molecular evolution of FOXP2, a gene involved in speech and language. *Nature* **418,** 869–872 (2002).
5. Zhang, J., Webb, D. M. & Podlaha, O. Accelerated protein evolution and origins of human-specific features: Foxp2 as an example. *Genetics* **162,** 1825–1835 (2002).
6. Spiteri, E. *et al.* Identification of the transcriptional targets of FOXP2, a gene linked to speech and language, in developing human brain. *Am. J. Hum. Genet.* **81,** 1144–1157 (2007).
7. Vernes, S. C. *et al.* High-throughput analysis of promoter occupancy reveals direct neural targets of FOXP2, a gene mutated in speech and language disorders. *Am. J. Hum. Genet.* **81,** 1232–1250 (2007).
8. Li, S., Weidenfeld, J. & Morrisey, E. E. Transcriptional and DNA binding activity of the Foxp1/2/4 family is modulated by heterotypic and homotypic protein interactions. *Mol. Cell. Biol.* **24,** 809–822 (2004).
9. Oldham, M. C. *et al.* Functional organization of the transcriptome in human brain. *Nature Neurosci.* **11,** 1271–1282 (2008).
10. Zhang, B. & Horvath, S. A general framework for weighted gene co-expression network analysis. *Stat. Appl. Genet. Mol. Biol.* **4,** 17 (2005).
11. Acampora, D. *et al.* Craniofacial, vestibular and bone defects in mice lacking the Distal-less-related gene *Dlx5*. *Development* **126,** 3795–3809 (1999).
12. Yoshihara, M., Adolfsen, B., Galle, K. T. & Littleton, J. T. Retrograde signaling by Syt 4 induces presynaptic release and synapse-specific growth. *Science* **310,** 858–863 (2005).
13. Brusse, E. *et al.* Spinocerebellar ataxia associated with a mutation in the fibroblast growth factor 14 gene (SCA27): A new phenotype. *Mov. Disord.* **21,** 396–401 (2006).
14. Holmes, S. E. *et al.* Expansion of a novel CAG trinucleotide repeat in the 5′ region of PPP2R2B is associated with SCA12. *Nature Genet.* **23,** 391–392 (1999).
15. Belton, E., Salmond, C. H., Watkins, K. E., Vargha-Khadem, F. & Gadian, D. G. Bilateral brain abnormalities associated with dominantly inherited verbal and orofacial dyspraxia. *Hum. Brain Mapp.* **18,** 194–200 (2003).
16. Shu, W. *et al.* Altered ultrasonic vocalization in mice with a disruption in the *Foxp2* gene. *Proc. Natl Acad. Sci. USA* **102,** 9643–9648 (2005).
17. Van Camp, G. *et al.* A new autosomal recessive form of Stickler syndrome is caused by a mutation in the *COL9A1* gene. *Am. J. Hum. Genet.* **79,** 449–457 (2006).
18. Uhlenberg, B. *et al.* Mutations in the gene encoding gap junction protein α12 (connexin 46.6) cause Pelizaeus-Merzbacher-like disease. *Am. J. Hum. Genet.* **75,** 251–260 (2004).
19. Johnson, M. B. *et al.* Functional and evolutionary insights into human brain development through global transcriptome analysis. *Neuron* **62,** 494–509 (2009).
20. Prabhakar, S., Noonan, J. P., Paabo, S. & Rubin, E. M. Accelerated evolution of conserved noncoding sequences in humans. *Science* **314,** 786 (2006).
21. Dorus, S. *et al.* Accelerated evolution of nervous system genes in the origin of *Homo sapiens*. *Cell* **119,** 1027–1040 (2004).
22. Enard, W. *et al.* A humanized version of Foxp2 affects cortico-basal ganglia circuits in mice. *Cell* **137,** 961–971 (2009).
23. Kumar, S. & Hedges, S. B. A molecular timescale for vertebrate evolution. *Nature* **392,** 917–920 (1998).
24. King, M. C. & Wilson, A. C. Evolution at two levels in humans and chimpanzees. *Science* **188,** 107–116 (1975).
25. Enard, W. *et al.* Intra- and interspecific variation in primate gene expression patterns. *Science* **296,** 340–343 (2002).
26. Caceres, M. *et al.* Elevated gene expression levels distinguish human from non-human primate brains. *Proc. Natl Acad. Sci. USA* **100,** 13030–13035 (2003).
27. Coppola, G. *et al.* Gene expression study on peripheral blood identifies progranulin mutations. *Ann. Neurol.* **64,** 92–96 (2008).

Supplementary Information is linked to the online version of the paper at www.nature.com/nature.

Acknowledgements We thank M. Oldham for generating the Illumina microarray mask file; J. Ou and E. Spiteri for performing site-directed mutagenesis; L. Chen for technical assistance; and L. Kawaguchi for laboratory management. Human tissue was obtained from the NICHD Brain and Tissue Bank for Developmental Disorders at the University of Maryland (NICHD Contract numbers N01-HD-4-3368 and N01-HD-4-3383). The role of the NICHD Brain and Tissue Bank is to distribute tissue, and therefore cannot endorse the studies performed or the interpretation of results. This work was supported by grant R21MH075028, R37MH60233-06A1 (D.H.G.), T32HD007032, an A.P. Giannini Foundation Medical Research Fellowship, and a NARSAD Young Investigator Award (G.K.), T32MH073526 (K.W.) NIH/NCRR grant RR00165 and a James S. McDonnell Foundation grant, JSMF 21002093 (T.M.P.).

Author Contributions G.K. and D.H.G. designed the study, analysed the data and wrote the paper; G.K. performed all of the experiments; J.M.B. made contributions to an earlier phase of the project including generating cell lines, immunoblotting and qRT–PCR; K.W. performed statistical analysis and weighted gene coexpression network analysis; G.C. conducted promoter analysis and G.C. and F.G. analysed the microarray data; Z.O.J. and J.A.W. performed mass spectrometry; S.P. performed some of the qRT–PCR; T.M.P. performed tissue dissections and provided non-human primate samples; all authors discussed the results and commented on the manuscript.

Author Information Gene expression data have been deposited in the NCBI Gene Expression Omnibus (GEO; http://www.ncbi.nlm.nih.gov/geo) and are accessible using GEO series accession number GSE18142. Reprints and permissions information is available at www.nature.com/reprints. Correspondence and requests for materials should be addressed to G.K. (gena@alum.mit.edu) or D.H.G. (dhg@ucla.edu).

METHODS

Antibodies. The following antibodies were either used for immunoblotting (IB) or immunofluorescence (IF): anti-Flag (mouse monoclonal, Sigma; 1:10,000 (IB), 1:10,000 (IF)), anti-GAPDH (mouse monoclonal, Chemicon; 1:2500 (IB)), anti-β-tubulin (rabbit polyclonal, Abcam; 1:1000 (IB)), anti-FOXP1 (ref. 6; 1:5000 (IB), 1:1000 (IF)), anti-CACNB2 (mouse monoclonal, Abcam; 1:100 (IB)), anti-ENPP2 (rabbit polyclonal, Cayman Chemical; 1:400 (IB)), goat anti-rabbit horseradish peroxidase (Cell Signaling, 1:2,500), goat anti-mouse horseradish peroxidase (Chemicon, 1:5,000), goat anti-mouse Alexa Fluor 488 (Invitrogen, 1:1,500), goat anti-rabbit Alexa Fluor 594 (Invitrogen, 1:1,500).

Cell culture and stable line generation. Stable SH-SY5Y cell lines were generated by transfecting cells with pCMV-Tag4a expression constructs using FuGENE (Roche Applied Science) according to the manufacturer's instructions. Populations of stable cells were selected using 1 mg ml^{-1} geneticin (Invitrogen). Multiple independent lines were generated from independent transfections. Stable human fetal neuronal progenitor cell lines were generated by transducing cells with lentiviruses as previously described[28]. FOXP2-producing lentiviral vectors were generated by replacing the eGFP in pLUGIP (ATCC) with FOXP2.

Immunoprecipitation. Nuclear extract was incubated with either 1 μg of Flag antibody (Sigma) or a polyclonal FOXP1 antibody[6].

Cell proliferation assay. Equal numbers of cells (2.0×10^4) were plated on time zero and counted every subsequent day after trypsinization using a haemacytometer.

Dual luciferase assays. 293T cells (ATCC) were transfected with 50 ng of reporter construct expressing *Photinus pyralis* (firefly) luciferase, 1 ng of *Renilla* luciferase plasmid (pRL-EF), and 50 ng of pCMV-Tag4a FOXP2 expression plasmid using FuGENE (Roche Applied Science) according to the manufacturer's instructions. Forty-eight hours later, cells were lysed and analysed using the dual luciferase reporter assay system (Promega) according to the manufacturer's instructions. Co-transfection of Renilla was used for transfection normalization, and values were additionally normalized to cells transfected with a promoter-less luciferase construct. Promoter information is in Supplementary Table 6. The canonical FOXP2 binding site driving luciferase was generated by cloning AATTTG in triplicate into pGL4 (Promega).

Gene ontology analysis. GO analysis was performed as described[6] using DAVID (http://david.abcc.ncifcrf.gov). The differentially expressed genes were compared to all of the genes on the microarrays and a *P* value computed using a Fisher's exact test.

Immunoblotting. Whole-cell protein lysates were generated and immunoblotted as described[28].

Immunofluorescence. Cells were grown on glass coverslips, fixed in 2% paraformaldehyde, and permeabilized in 0.2% Triton X-100. TBST containing 10% milk and 10% normal goat serum was used as blocking solution at room temperature for 1 h. Antibodies were diluted in TBS with 0.25% BSA, 0.25% normal goat serum and 0.1% Triton X-100 and applied to cells overnight at 4 °C. Secondary antibodies were diluted in blocking solution and added at room temperature for 1 h. Coverslips were mounted to glass slides and images taken using a Zeiss Axio Imager D1.

Mass spectrometry. FOXP2 immunoprecipitates were precipitated by the addition of trichloroacetic acid and proteolysed by the sequential addition of Lys-C and trypsin proteases[29]. Digested peptide samples were then analysed by mass spectrometry as described[29]. Proteins were considered to be present in a sample if at least two peptides per protein were identified using a false positive rate of less than 5% per peptide as determined using a decoy database strategy[30].

Microarrays. For the SH-SY5Y data, we analysed four biological replicates of each genotype from three independently generated cell lines for a total of 12 microarrays per genotype. Each of these cell lines was created from populations of cells rather than single clones, and as such, the expression data represent changes from hundreds of independent integrations throughout the cells' genomes. Furthermore, as the endogenous FOXP2 expression is very low in SH-SY5Y cells, the potential confound of heterodimerization with endogenous human FOXP2 is mitigated in these cells. For the tissue data, we analysed three to six independent samples for each brain region in each species. Detailed code for the microarray analysis is available[31].

Permutation testing. For FOXP2 correlations, we computed the average correlation for each gene on the microarray to either the level of the human or the chimpanzee FOXP2. We then derived the absolute difference in correlation for each gene between the human and chimpanzee FOXP2 arrays. The average of these differences was not statistically different from performing the same test while randomizing the correlation values for all of the genes on the arrays, or using the values from only the differentially expressed genes. For promoter binding site calculations, we calculated the number of promoters from differentially expressed genes with a given motif and compared them to the average number from a random selection of the same number of promoters from the genome. We assumed a normal distribution and a *Z*-score less than 0.05 was called significant. Similar analysis was done for comparing genes with a haCNS and expression in human fetal brain. For microarray overlap comparisons, we included the number of differentially expressed genes as well as the total number of probe sets on the microarrays for each comparison. We used a hypergeometric distribution test with 10,000 permutations to calculate the mean and standard deviation of the overlap. We assumed a normal distribution, and a *Z*-score less than 0.05 was called significant.

Real-time PCR. RNA extraction and RT–PCR was performed as described[6]. Primer sequences are in Supplementary Table 10.

Site-directed mutagenesis. Mutagenesis of pCMV-Tag4a/FOXP2[6] was carried out using the GeneTailor Site-Directed Mutagenesis System (Invitrogen) according to the manufacturer's instructions using the following primers: site 1 (asparagine to threonine), F-5′-CCTCCTCGACTACCTCCTCCACAACTTCCAAAGC-3′, R-5′-GGAGGAGGTAGTCGAGGAGGAATTGTTAGTA-3′; site 2 (serine to asparagine), F-5′-ATGGACAGTCTTCAGTTCTAAACGCAAGACGAGA-3′, R-5′-TAGAACTGAAGACTGTCCATTCACTATGGAA-3′. Mutagenesis was confirmed by both sequencing and mass spectrometry.

Weighted gene coexpression network analysis (WGCNA). WGCNA was performed as previously described[9,10]. Briefly, genes were chosen for inclusion into the network on the basis of their consistent presence on the array and high coefficient of variation, and they were clustered based on their topological overlap. For each module, singular value decomposition ($X = UDV'$) was performed, and the expression was re-calculated without the first principal component because it corresponded to cell line differences. The modules reported in this study were created using expression data with the first principal component removed, as it represented an experimental batch effect.

28. Konopka, G., Tekiela, J., Iverson, M., Wells, C. & Duncan, S. A. Junctional adhesion molecule-A is critical for the formation of pseudocanaliculi and modulates E-cadherin expression in hepatic cells. *J. Biol. Chem.* **282**, 28137–28148 (2007).
29. Wohlschlegel, J. A. Identification of SUMO-conjugated proteins and their SUMO attachment sites using proteomic mass spectrometry. *Methods Mol. Biol.* **497**, 33–49 (2009).
30. Elias, J. E. & Gygi, S. P. Target-decoy search strategy for increased confidence in large-scale protein identifications by mass spectrometry. *Nature Methods* **4**, 207–214 (2007).
31. Coppola, G., Winden, K., Konopka, G., Gao, F. & Geschwind, D. H. Expression and network analysis of Illumina microarray data. *Nature Protocols* doi:10.1038/nprot.2009.215 (2009).